GLIA 33:256–266 (2001)

Dynamics of Microglial Activation: A Confocal Time-Lapse Analysis in Hippocampal Slices

NICK STENCE, MARC WAITE, AND MICHAEL E. DAILEY*
Department of Biological Sciences, University of Iowa, Iowa City, Iowa

KEY WORDS microglia; motility; confocal imaging; brain slice; hippocampus

ABSTRACT The dynamics of microglial cell activation was studied in freshly prepared rat brain tissue slices. Microglia became activated in the tissue slices, as evidenced by their conversion from a ramified to amoeboid form within several hours in vitro. To define better the cytoarchitectural dynamics underlying microglial activation, we performed direct three-dimensional time-lapse confocal imaging of microglial cells in live brain slices. Microglia in tissue slices were stained with a fluorescent lectin conjugate, FITC-IB_4, and stacks of confocal optical sections through the tissue were collected repeatedly at intervals of 2–5 min for several hours at a time. Morphometric analysis of cells from time-lapse sequences revealed that ramified microglia progress to amoeboid macrophages through a stereotypical sequence of steps. First, in the withdrawal stage, the existing ramified branches of activating microglia do not actively extend or engulf other cells, but instead retract back (mean rate, 0.5–1.5 μm/min) and are completely resorbed into the cell body. Second, in the motility stage, a new set of dynamic protrusions, which can exhibit cycles of rapid extension and retraction (both up to 4 μm/min), abruptly emerges. Sometimes new processes begin to emerge even before the old branches are completely withdrawn. Third, in the locomotory stage, microglia begin translocating within the tissue (up to 118 μm/h) only after the new protrusions emerge. We conclude that the rapid conversion of resting ramified microglia to active amoeboid macrophages is accomplished not by converting quiescent branches to dynamic ones, but rather by replacing existing branches with an entirely new set of highly motile protrusions. This suggests that the ramified branches of resting microglia are normally incapable of rapid morphological dynamics necessary for activated microglial function. More generally, our time-lapse observations identify changes in the dynamic behavior of activating microglia and thereby help define distinct temporal and functional stages of activation for further investigation. *GLIA 33:256–266, 2001.*

INTRODUCTION

Microglia are a class of resident glial cells that play key roles in mediating responses to CNS tissue injury in a wide variety of pathological conditions (Kreutzberg, 1996; González-Scarano and Baltuch, 1999). Accumulating evidence suggests that microglia play either neuroprotective or cytotoxic roles, depending on the severity of tissue injury (Benati et al., 1993; Aschner et al., 1999; Bruce-Keller, 1999). It has long been evident that microglia exhibit different morphological forms following CNS injury (Nissl, 1899; del Rio-Hortega, 1932), and each form is thought to subserve a distinct functional role (Davis et al., 1994; Raivich et al., 1999). In the mature, uninjured CNS, microglia are highly branched or ramified. This so-called resting form is presumed to exhibit little move-

To obtain the stereo glasses for viewing figures 1, 5, and 6, please contact Dr. Michael E. Dailey. See address below.

Grant sponsor: American Cancer Society seed grant administered through the University of Iowa Cancer Center; Grant number: IN-122R.

*Correspondence to: Dr. Michael E. Dailey, Department of Biological Sciences, 335 Biology Building, University of Iowa, Iowa City, IA 52242.
E-mail: michael-e-dailey@uiowa.edu

Received 14 July 2000; Accepted 10 October 2000

ment and structural change, although they may be actively involved in immune surveillance (Kreutzberg, 1996) and extracellular fluid cleansing (Thomas, 1992). In response to neural tissue injury, microglia are activated and undergo a graded but stereotypical program of morphological and molecular changes that is proportionate to the severity of tissue injury (Kreutzberg, 1996; Raivich et al., 1999). Activated microglia become deramified and develop an enlarged cell body with several short, thickened processes. This morphological transformation can occur within hours of initial activation and coincides with microglial homing and adhesion to damaged neurons (Kloss et al., 1999; Raivich et al., 1999). If tissue damage is extensive, microglia develop an amoeboid appearance and become phagocytic. Amoeboid cells may be converted to a reactive form that exhibits a spheroid shape with few processes but retains phagocytic activity. Activated and reactive forms may eventually return to a resting, ramified state (Hailer et al., 1996, 1997b). Thus, the distinct morphological forms arise by interconversion within a common set of cells, yielding a stereotypical sequence of morphological changes following activation.

A central tenet implicit in models of microglial function is that the conversion from a resting, ramified form to an activated form is essential for expression of the full repertoire of microglial functions. Activated microglia move rapidly to focal sites of injury (McGlade-McCulloh et al., 1989), where they proliferate, engage dead/damaged cells, remove debris by phagocytosis, and present antigen to infiltrating lymphocytes (Raivich et al., 1998, 1999). Time-lapse studies of microglia in cell culture (Booth and Thomas, 1991; Ward et al., 1991; Haapaniemi et al. 1995; Tomita et al., 1996; Takeda et al., 1998) and rodent brain slices (Smith et al., 1990; Brockhaus et al., 1996) have shown that amoeboid microglia are indeed capable of highly active movements that enable migration and phagocytosis. However, there is little information on how ramified cells are initially transformed into mobile, macrophage-like cells. Such early activation events are difficult to study directly because static images from fixed tissues cannot capture changes in functional behavior of cells, and the process of isolating live microglia for in vitro study disrupts their native setting. To circumvent these problems, we combined vital fluorescence staining and time-lapse confocal imaging in an acute brain slice preparation that preserves the native structure and organization of microglia. We use this approach to define the sequence of dynamic morphological and functional changes during early stages of microglial activation in mammalian brain tissue.

MATERIALS AND METHODS

Tissue Slice Preparation and Culture

Tissue slices were prepared from early postnatal (P3–P14) rat hippocampus as described in detail elsewhere (Dailey and Waite, 1999). Briefly, rats were euthanized according to institutional guidelines, brains were removed and placed in ice-old Hanks balanced salt solution (HBSS), and hippocampi were dissected free. Hippocampi were sliced transversely at a thickness of 400 μm using a manual tissue chopper, and slices were either fixed immediately for subsequent staining and observation; immediately stained and mounted for time-lapse observation; or cultured briefly (1-24 h) using either the roller tube (Gähwiler et al., 1997) or static filter culture technique (Stoppini et al., 1991). Tissue slices from early postnatal animals were used because the immature neural tissue survives much better in vitro than tissues from more mature animals. The region adjacent to the hippocampal fissure near the dentate gyrus is rich in microglia (Dalmau et al., 1998), and many of the observations described in this study were derived from this area. However, qualitatively similar observations were made from other hippocampal regions.

Fluorescent Labeling of Microglia

The B_4 isolectin from *Griffonia simplicifolia* seeds has been shown to be a useful marker of microglia in many CNS tissues (Streit and Kreutzberg, 1987; Streit, 1990; Boya et al., 1991). IB_4 also labels endothelial cells of blood vessels, but these long tubular structures are usually easily distinguished from microglia. For fluorescence visualization of microglia, tissue slices were stained with fluorescein (FITC)-labeled IB_4 (FITC-IB_4; Sigma, St. Louis) as described in detail elsewhere (Dailey and Waite, 1999). A stock solution of FITC-IB_4 was prepared in water at 200 μg/ml and stored as frozen (−20°C) aliquots (200 μl/aliquot). A final working solution (5 μg/ml) was prepared from the stock immediately prior to use. For high-resolution three-dimensional (3D) reconstruction, tissue slices were fixed in culture media or HBSS containing 4% paraformaldehyde for at least 1 h, then rinsed briefly before applying FITC-IB_4 for 1 h to 3 days. The longer incubation times often improved dye penetration to deeper portions of the thick tissue slices. For live cell imaging, tissues were incubated in culture media containing FITC-IB_4 (5–15 μg/ml) for 15 min to 2 h, rinsed with dye-free media (5 min), then mounted in fresh HEPES-buffered media. In some cases, FITC-IB_4 was included in the dissection media in order to minimize the time between animal sacrifice and imaging.

Confocal Microscopy and Analysis

Fluorescently stained tissue samples were imaged using a Leica TCS NT scanning laser confocal microscope (Leica) equipped with Argon (Ar; 488 nm), Krypton (Kr; 568 nm), and Helium-Neon (HeNe; 633 nm) lasers. Microglia stained with FITC-IB_4 were visualized with a fluorescein filter set (515 nm dichroic mirror, 530 nm long-pass barrier filter) using Argon laser

(488 nm) illumination. The microscope objectives used in these studies included a 10×/0.3 PL FLUOTAR, a 20×/0.5 PL FLUOTAR, a 25×/0.75 oil FLUOTAR, and a 63×/1.2 water PLAN APO (all Leica). Digital images were captured by the confocal host computer (Pentium Pro 200), temporarily stored on a Windows NT 4.0 network server (18 GB) then archived onto CD.

Three-dimensional volume rendering

For 3D confocal reconstruction of microglia in fixed tissue slices, z-stacks of 40 to 200 optical sections (1,024 × 1,024 pixel array) were collected using the computer-controlled microstepper stage of the confocal microscope. The x-, y-, and z-voxel dimensions were between 0.15 and 0.4 μm. To maintain high axial spatial resolution and improve the signal-to-noise ratio in the confocal image, the detector pinhole aperture was set to one to two times the size of the Airy disc, and two to eight scans were averaged for each optical section. The 63× water PLAN APO objective, with long working distance (220 μm) and high numerical aperture (1.2), was especially useful for collecting high-resolution 3D image stacks. To render cells in three dimensions, we used the software program Voxblast (developed at the University of Iowa Image Analysis Facility) running on a 350 MHz Pentium II PC. Stacks of images were loaded, a threshold grayscale level was set to best match the outline of the cell of interest, and a 3D volume was rendered. Stereo pairs of images (e.g., Fig. 1B) were generated by color-encoding two different images representing slightly different visual perspectives (10° rotation difference).

Time-lapse imaging

For time-lapse imaging, tissue slices were mounted in a closed chamber with HEPES-buffered culture media (0.5–1 ml, pH 7.3) and maintained on the microscope stage heated (35°C) by forced warm air, as described elsewhere (Dailey, 1999). To avoid evaporation of the immersion medium when using the 63× water immersion objective with forced air stage heating, we used a synthetic refractive index liquid (N.D. 1.335; McCrone Accessories, Westmont, IL) with refractive properties close to that of water. Time-lapse imaging of live, FITC-IB_4–stained tissue slices commenced within 30–90 min (usually 60–75 min) of decapitation.

To image cells in three dimensions within live tissue slices, stacks of confocal optical sections were collected at 2- to 5-min intervals. Such volume imaging provided a means for observing the 3D structure and movements of live cells within the tissue volume. Each stack was composed of 8 to 18 optical sections (512 × 512 or 1,024 × 1,024 pixel arrays, two or three scans averaged per optical section) spanning up to 60 μm in the axial (z) dimension. For imaging relatively large tissue volumes and fields of view, a dry 20× objective (960 μm working distance) was used. With the pinhole set at two to three times the Airy disk, the optical section thickness of the 20× objective permitted axial spacing of z-sections from 3 to 6 μm apart while still providing adequate representation and reconstruction of the cells.

Quantifying morphological changes

For quantifying morphological parameters including cell body diameter, rates of locomotion, and changes in length of microglial processes, stacks of optical sections for each time point were combined into a single two-dimensional (2D) projection image using a custom-written Pascal script running in Scion Image beta3b (Scion, Frederick, MD). Photoshop 5.0 (Adobe Systems) was used to automate adjustments in brightness and contrast and to reduce noise in the image by Gaussian blur filtering. Measurements were made in the 2D projection images using the measure tool in Scion Image. Lateral drift in the field of view was corrected for by reference to a stable, fiduciary structure in the image. Measurements were exported to Microsoft Excel for computation, analysis, and graphic display. The final graphic output (e.g., Fig. 2) was composed in CorelDraw 6 (Corel, Ottawa). Measures of microglial process length, rates of process elongation/retraction, and cell locomotion may be slight underestimates because they are based on 2D projections of 3D data sets.

Generating 3D movies

To generate 3D movies of imaged tissue volumes, left and right stereo projection images were constructed for each time point in an automated fashion using Scion Image. For viewing the 3D time-lapse sequences, the red-green composite images were assembled into AVI or QuickTime format digital movies using Premiere 5.1 (Adobe). Depth in the stereo images is viewed using red-green stereo glasses (American Paper Optics, Bartlett, TN).

RESULTS

Microglia Activate Rapidly in Rat Hippocampal Tissue Slices

The very process of preparing live brain tissue slices activates microglia within the slices, probably as a consequence of mechanical injury or death of some neurons during the tissue slicing procedure (Hailer et al., 1996; Dailey and Waite, 1999). To define better the dynamic morphological changes in microglia during and following activation, we examined tissue slices fixed either immediately after dissection or following a brief (1 to 24 h) culture period. Confocal imaging of FITC-IB_4–stained tissue slices that were fixed immediately after preparation showed intense labeling of

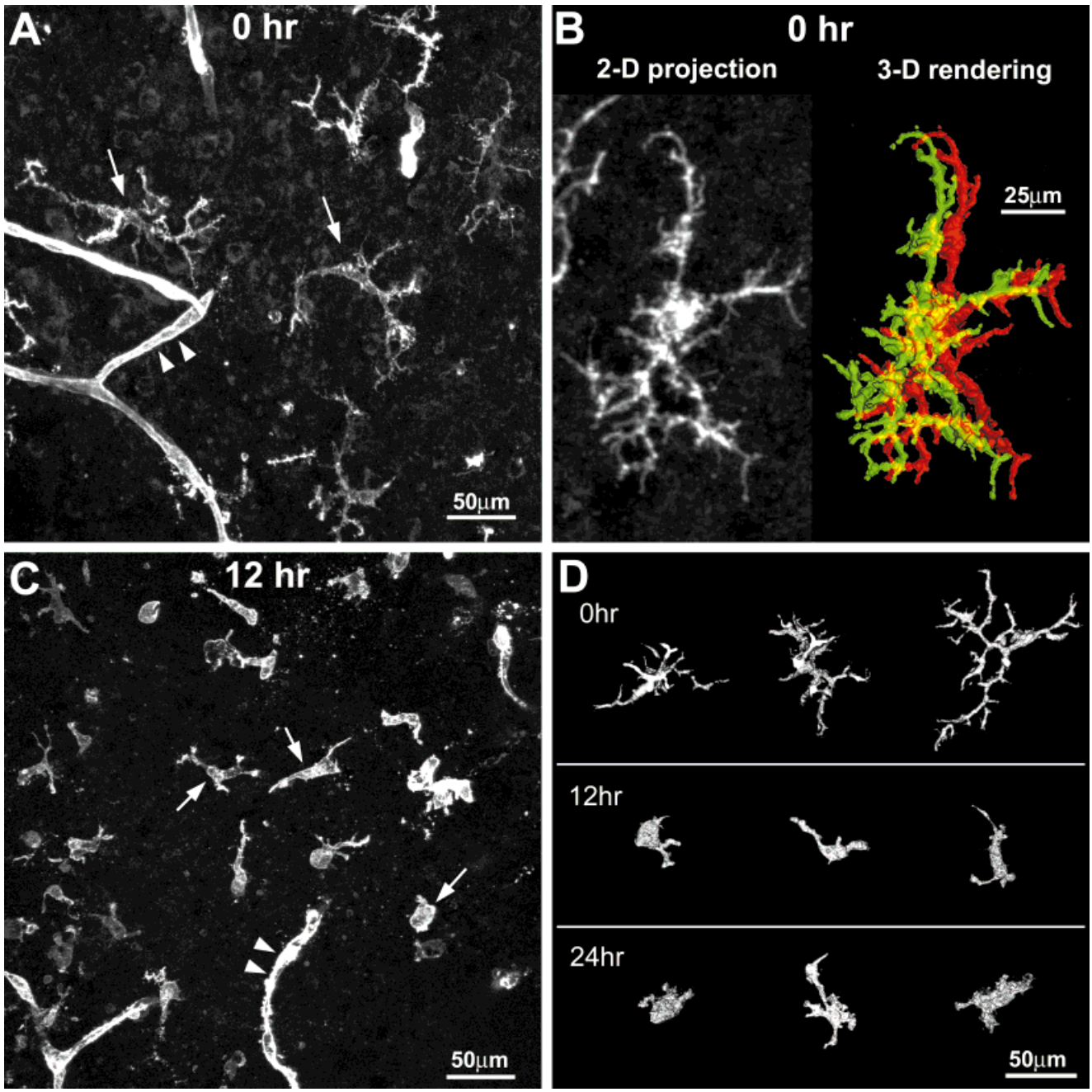

Fig. 1. Microglia in acutely isolated tissue slices transform from a highly ramified to amoeboid-like morphology within several hours. **A:** Microglia initially have long, ramified branches. This 2D projection image, which represents a stack of 197 confocal optical sections through 63 μm of depth, shows the full branching pattern of ramified microglial cells (arrows) in a hippocampal slice fixed immediately after slicing. Microglia were stained with FITC-IB_4, which also labels blood vessels (arrowheads). **B:** Higher magnification views of a cell more clearly show that microglia in acutely prepared slices are highly branched. Note the fine, finger-like extensions emanating from the major branches. The 2D projection image and 3D surface rendering of the same cell were generated from a stack of 74 confocal optical sections spanning 29 μm in the axial dimension. To view depth in the 3D image, place the red pane of red-green stereo glasses over left eye. **C:** By 12 h in vitro, microglia (arrows) have lost most of their branches and appear amoeboid in form. This 2D projection image represents 51 optical sections through 20 μm in depth. **D:** 3D renderings of representative microglia in slices fixed at different stages more clearly show the reduction in number and length of branches within the first 12 h in vitro. The overall morphology of the cells changes little over the subsequent 12 h. All images in this figure are from tissues originally derived from P6 animals.

branched cells scattered throughout the tissue (Fig. 1A). Three-dimensional reconstruction of tissue volumes from confocal optical sections better revealed that IB_4-stained cells are highly branched, having usually two to six primary branches (some $>$ 50 μm long) that radiate from the soma and that have many thin, finger-like protrusions which extend from the primary branches (Fig. 1B). These cells closely resemble the

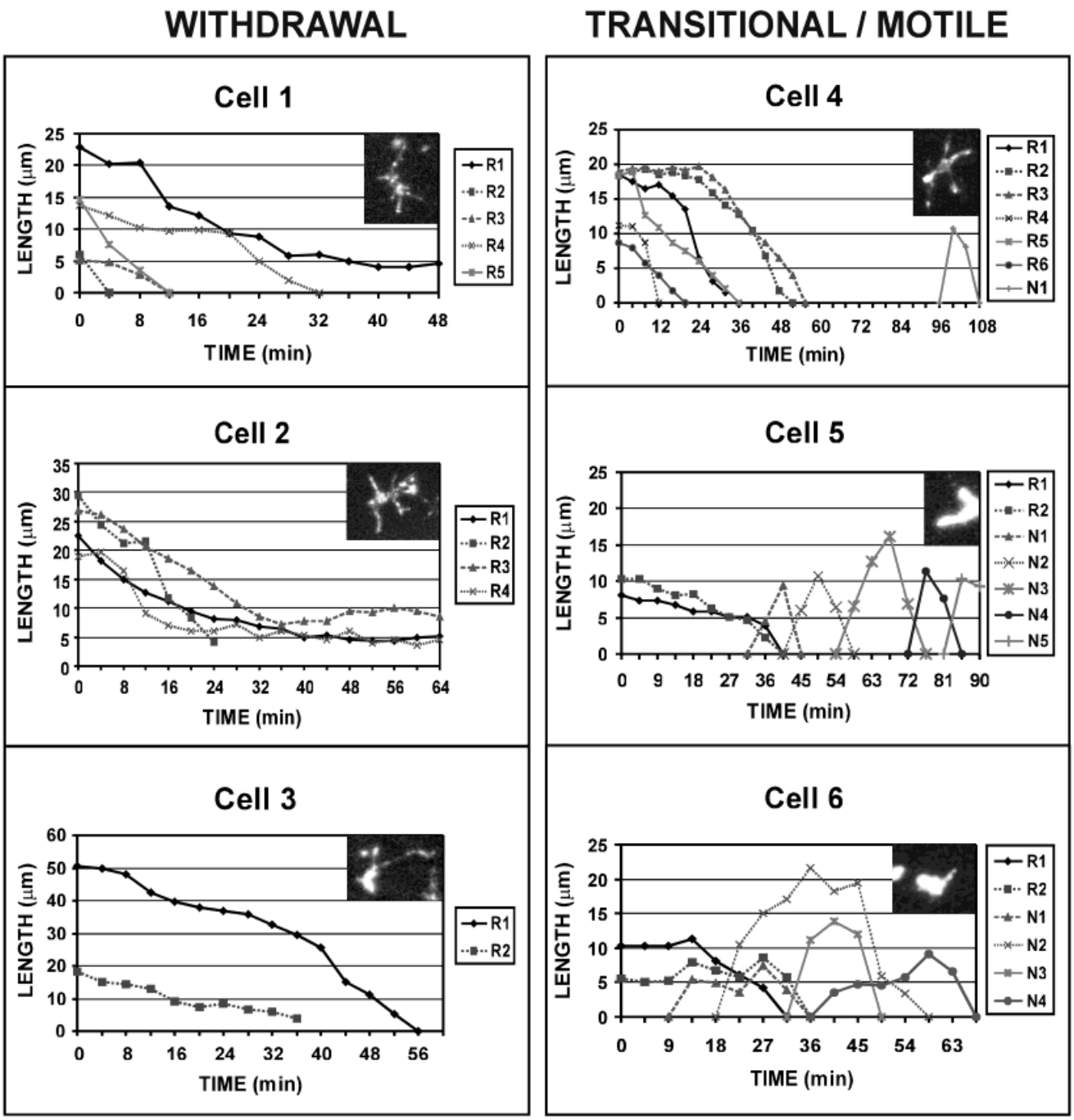

Fig. 2. Graphic representation of the dynamics of microglial cell branches during withdrawal and transition to a highly motile stage. The lengths of all of the individual processes on six representative cells (two cells from each of three slices) were plotted for each time point. Individual retracting branches are designated R1, R2, etc., while new protrusions are designated N1, N2, etc. An image of each cell at time zero is shown. By the start of each time sequence, the cells had been activated and are in the process of withdrawing their branches. Cells 1–3 withdrew their processes at typical rates of 0.5–1.5 μm/min, but these cells did not immediately generate new protrusions. Cells 4–6 withdrew their processes and began to generate new protrusions, the timing of which was variable from cell to cell. For cell 4, some branches (e.g., R4, R6) retracted completely before other branches (e.g., R2, R3) began to retract. Note also that the delay between branch withdrawal and new protrusion was over 40 min. Cells 5 and 6 began to generate new protrusions during the final stages of branch withdrawal. We refer to this period of overlap of withdrawal and new protrusion as the transitional stage (T-stage). Note that the newly generated protrusions grow and shrink rapidly and are much more dynamic than the initial, retracting branches. Time-lapse sequences for cells 4 through 6 are shown in Figures 3 through 5, respectively.

primitive ramified microglia or resting microglia described in the developing rat hippocampus in vivo (Dalmau et al., 1998).

Examination of tissue slices that were cultured for several hours before fixation revealed changes in the distribution and morphology of the IB_4-labeled cell popula-

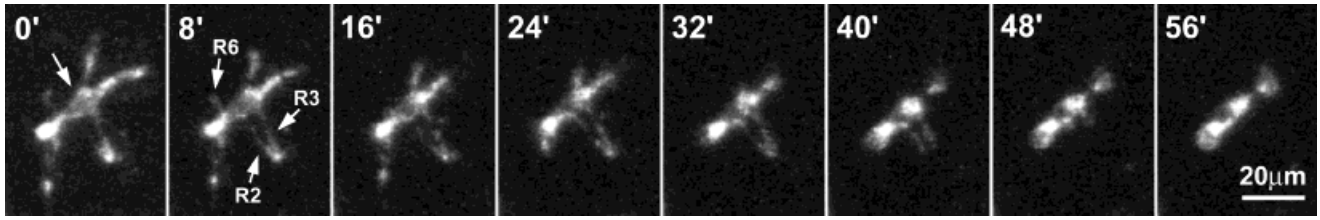

Fig. 3. Withdrawal stage: time-lapse confocal imaging demonstrates that activated microglia first retract all extant branches. The first time-point (0′) in the series was collected within 45 min of sacrificing the animal (postnatal day 5). All six of the major branches that were initially projecting from the cell body (arrow at 0′) were completely retracted within 1–2 h of sacrifice. Note that retracting process number 6 (R6) was fully resorbed into the cell body even before processes 2 and 3 (R2, R3) began to retract. The first new protrusion was formed ~ 45 min after completion of the withdrawal stage. The time series shows selected images, each of which is a composite of 10 optical sections, originally collected at 4-min intervals. See Figure 2 (cell 4) for a graphic representation of the retraction of these processes.

tion. By 12 h postsacrifice, virtually all IB_4-labeled cells had a morphology that is characteristic of activated microglia (Fig. 1C). Within 24 h, FITC-IB_4–labeled cells were highly concentrated on the surfaces of the tissue slices, although numerous microglial cells were also found scattered throughout the depth of the tissue. Volume rendering of microglia clearly demonstrated the rapid transformation from a ramified to an amoeboid-like morphology having fewer, stouter processes but with a larger perinuclear cytoplasmic volume (Fig. 1D). These observations from fixed tissue samples confirmed that microglial activation in hippocampal slices proceeds along a typical course and involve a rapid morphological transformation. However, they left unanswered questions about how the change in morphology is accomplished and how this may relate to a change in functional behavior of microglia.

Time-Lapse Imaging of Microglial Activation in Live Tissue Slices

To study directly the dynamic transformation of individual microglia during and following activation, we imaged freshly prepared FITC-IB_4–stained tissue slices by time-lapse confocal microscopy. The results reported here are based on time-lapse observations of over 200 cells in 50 tissue slices. Our time-lapse analysis revealed a step-wise progression in microglial cell behavior during activation. Not all microglia responded with the same time course, but there was a stereotypical sequence of dynamic morphological changes. In order to capture the earliest possible events, we attempted to minimize the time between animal sacrifice and imaging of the live, FITC-IB_4–stained tissue slices. At the earliest time point examined (30 min postsacrifice), most microglia were still ramified but were in the process of retracting their branches, the longest of which was typically 20–50 μm. The time course of retraction was variable from cell to cell but could last from just a few minutes to several hours, depending on the rate of retraction and the length of the branches. Branches on individual microglial cells often, but not always, retracted concomitantly. For example, some processes completely retracted before others had begun to retract (Fig. 3). Different branches on individual cells did not always retract at the same rate. Branches typically receded at a rate of 0.5–1.5 μm/min, but could show instantaneous retraction rates of up to 2.6 μm/min. Bulbous expansions were occasionally found at the tips of retracting branches, and these retraction bulbs grew somewhat larger as the tips of the retracting processes approached the cell body. This suggests that retracting processes are disassembled at their tips and that at least some of the cytoplasmic and/or membranous materials accumulate locally at the tips of the processes as they retract. Once at the cell body, the tips of the retracting processes were resorbed into the cell body. We refer to this first stage following activation as the withdrawal stage (W-stage), since the cells are uniformly withdrawing their branches from the surrounding tissue. We did not observe any significant, sustained growth of preexisting branches.

Following the withdrawal stage, many microglia make an abrupt transition to a more dynamic motility stage (M-stage) involving cycles of extension and retraction of new processes (Fig. 4). The transition from retracting (W-stage) to motile (M-stage) microglia was observed directly in over 40 cells. Microglia often did not move or generate any new protrusions until the old, ramified branches were completely resorbed, or nearly so. For some cells, the formation of new motile protrusions commenced only after a significant time delay (30 min or more) following the resorption of preexisting branches. However, other cells generated new protrusions during the final phase of process withdrawal, that is, once the old processes had retracted to within a length equal to approximately one cell body diameter (~ 10 μm). These cells had a transitional stage (T-stage), typically lasting 5–20 min, in which retraction of the old processes was occurring concomitant with the emergence of new processes. Regardless of when the new protrusions emerged, they were much more dynamic than the old processes: they grew at a rate of 1–4 μm/min, and for a given cell, they were also capable of retracting at a rate (up to 4 μm/min) that was three- to fourfold faster than the rate of retraction of the preexisting branches. In some cells (n = 12), the new pro-

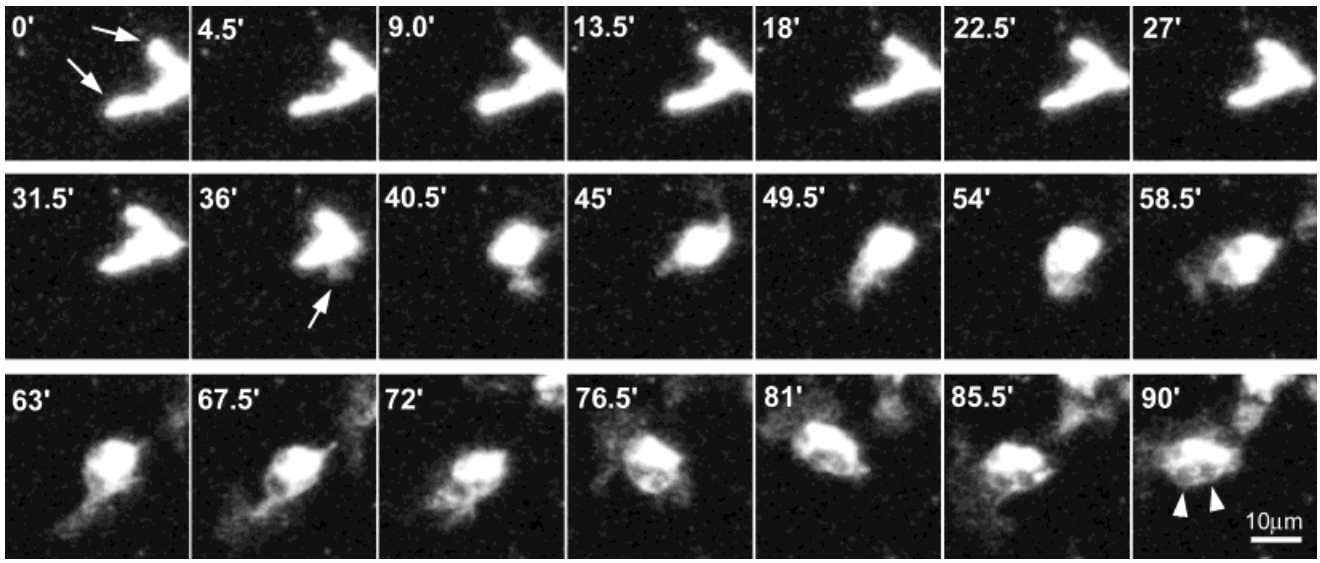

Fig. 4. Transition from withdrawal to motility stage. The final stage of ramified branch withdrawal produces irregularly shaped cells having a few stout processes (arrows at 0′). In some cells, new protrusions are rapidly generated (e.g., arrow at 36′) even before the initial branches are fully resorbed (40.5′). Note the rapid extension and retraction of new protrusions, some of which are flat sheet-like lamellae, whose motility can generate phagocytic vacuoles (arrowheads at 90′). The tissue is from a P10 rat. These images are composite projection images of 10 optical sections collected at 3 μm z-step intervals. A graphic representation of the branch dynamics is shown in Figure 2 (cell 5).

trusions began to form cup- or bubble-shaped profiles soon after their emergence (Fig. 5). The cup-shaped profiles appeared to surround other neighboring cells and either completely engulf the cells (Fig. 6A) or withdraw without forming enclosed vacuoles (Fig. 6B). In stark contrast, we never observed the old branches engaged in any of these dynamic behaviors, even when the old branches were found along side the new protrusions during the transition stage (T-stage). The distinct differences in dynamic behavior of microglial processes during the withdrawal, transitional, and motility stages are shown graphically in Figure 2.

Although activated microglia can become highly motile and can physically interact with neighboring cells in the tissue even as the cell body remains stationary, many cells do indeed begin to move through the tissue. Microglia in such a locomotory stage (L-stage) typically had a few lamellipodia-like processes that extended in different directions, but some cells had a polarized morphology with one prominent leading process. Regardless, the cells could move through the tissue very rapidly (up to 118 μm/h). Even as microglia moved through the tissue, they often extended several short, fleeting processes that protruded tangential to the primary direction of movement (Fig. 7). The lateral processes of the migrating microglia presumably enable direct physical contact with many cells within a short period of time, supporting a tissue surveillance function.

DISCUSSION

Our observations provide the first time-resolved morphological details of the transformation of resting, ramified microglia to active, amoeboid cells. The data support a multistep model of the early phase of microglial activation, which we summarize in Figure 8. The main finding is that the functional change in microglial behavior depends not on the conversion of quiescent ramified branches to a more dynamic state, but rather on a dramatic morphological transformation involving the replacement of the ramified branches with an entirely new set of highly motile protrusions. Thus, ramified microglia first retract their branches, then generate a new set of protrusions that support all of the dynamic activities of activated microglia. This extensive cellular reorganization coincides with an abrupt change in functional state that enables microglia to patrol injured neural tissue and to engage physically many cells rapidly.

Although these observations were made in isolated brain slices, the changes we observed over the first 24 h are consistent with the known sequelae of microglial activation following traumatic CNS tissue injury in vivo (Raivich et al., 1999). Activation of microglia in tissue slices is likely a response to neuronal trauma and cell death rather than direct mechanical injury to microglia. Some microglia at the slice surfaces were sufficiently damaged that they did not show the stereotypical morphological changes associated with activation, but most or all microglia in deeper tissue levels exhibited the stereotypical activation response.

The dynamic movements of cells we identify here as microglia are in general agreement with previous time-lapse studies of putative microglia in slices of rat hippocampus (Smith et al., 1990) and mouse corpus callosum and cingulum (Brockhaus et al., 1996). Those studies revealed populations of highly active cells that

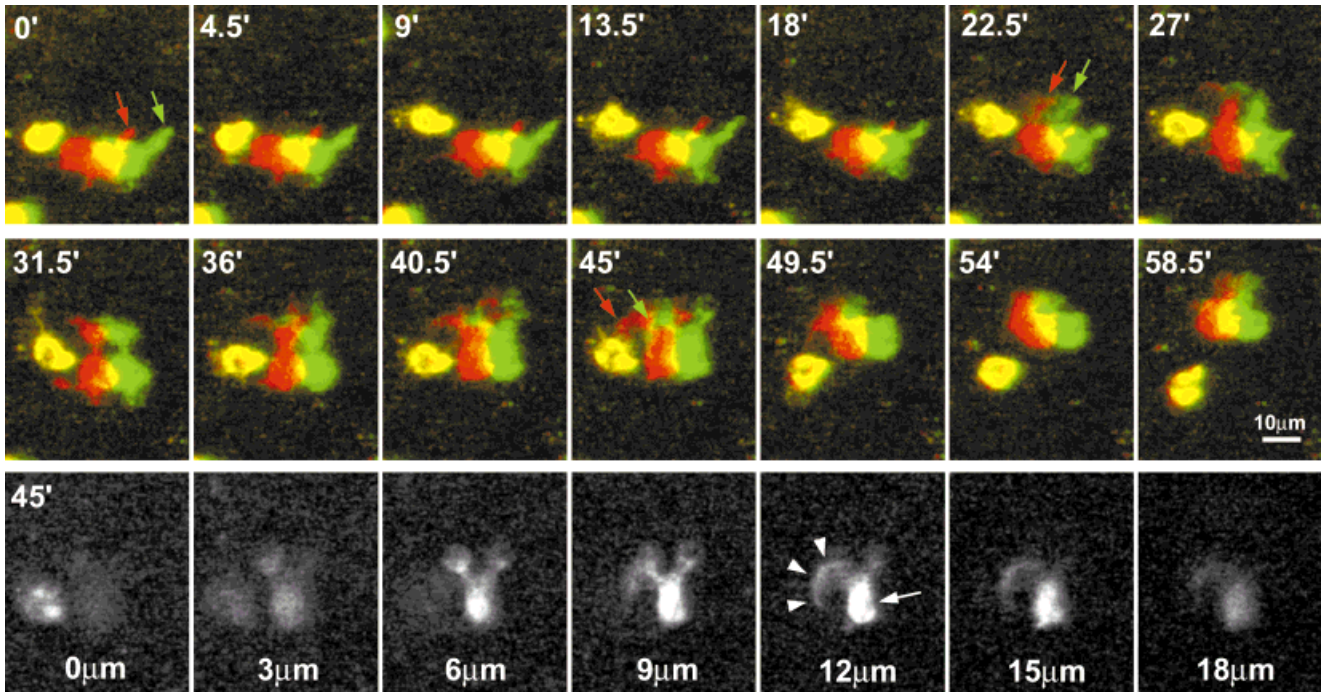

Fig. 5. Transition from withdrawal to motility stage. Red-green stereo time-lapse sequence (top two rows) shows final stages of retraction of a branch (arrow at 0′) and concomitant extension of a new process (arrow at 22.5′). The new protrusion immediately forms a bubble-like structure (arrow at 45′) that is likely to enclose an unlabeled cell or extracellular fluid. The bottom row shows selected images from the through-focus series of images taken at the 45′ time point to demonstrate more clearly the bubble-like structure (arrowheads at 12 μm) that extends from the microglial cell body (arrow). Tissue is from a P10 rat. Stereo images represent nine optical sections through 27 μm of depth. A graphic representation of the process dynamics is shown in Figure 2 (cell 6).

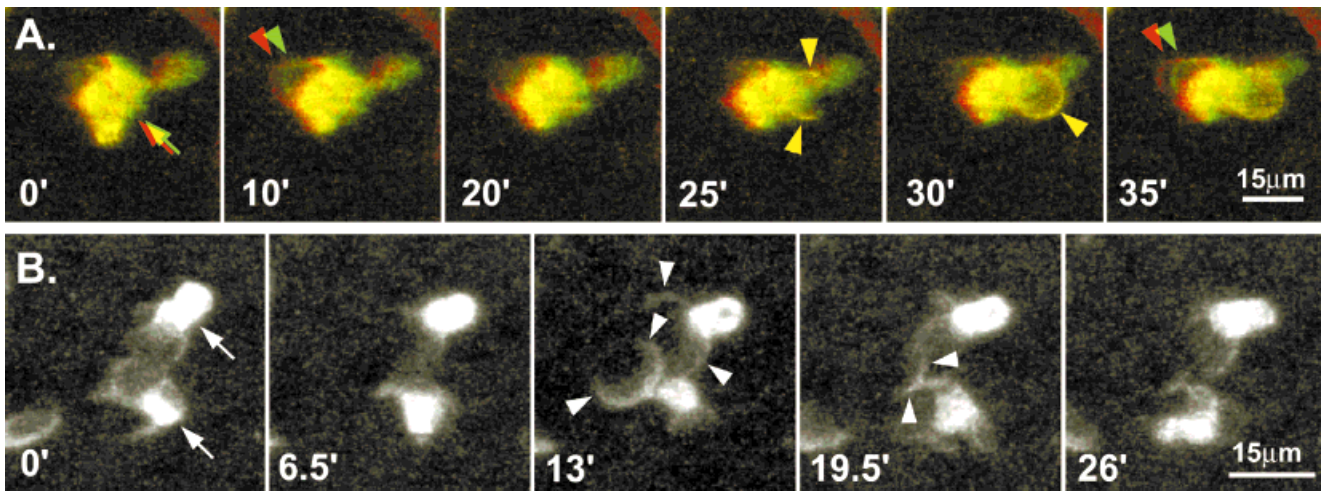

Fig. 6. New, highly dynamic processes form cup-like structures that develop into vacuoles or retract back without engulfing material. **A:** Red-green stereo time-lapse sequence shows a microglial cell body (arrow at 0′) containing a clear vacuole that persists throughout the time series (arrowheads at 10′ and 35′). The cell forms a new cup-like process (arrowheads at 25′) that rapidly develops into a bubble-like enclosure (arrowhead at 30′). This indicates that the microglial cell has engulfed some material, possibly a dead cell or cell debris resulting from damage during the tissue slicing. Tissue is from a P7 rat. Images represent eight optical sections through 26 μm of depth. **B:** Two activated microglia (arrows at 0′) form cup-like protrusions (arrowheads at 13′) in a tissue slice from a P6 rat. The bottom cell retracts its processes (arrowheads at 19.5′) from around the spheroid object rather than ingesting the object. We refer to this transient ensheathing activity as frisking. Each image represents a composite of eight optical sections through 30 μm of tissue depth.

were capable of moving to the surface of the tissue slices and phagocytosing other dead and damaged cells. From their observations, Brockhaus et al. (1996) concluded that highly active microglia are unique to the cingulum and corpus callosum since similar active microglia were not found in slices from hippocampus or other brain regions. Moreover, it was suggested that the observed amoeboid microglia did not become acti-

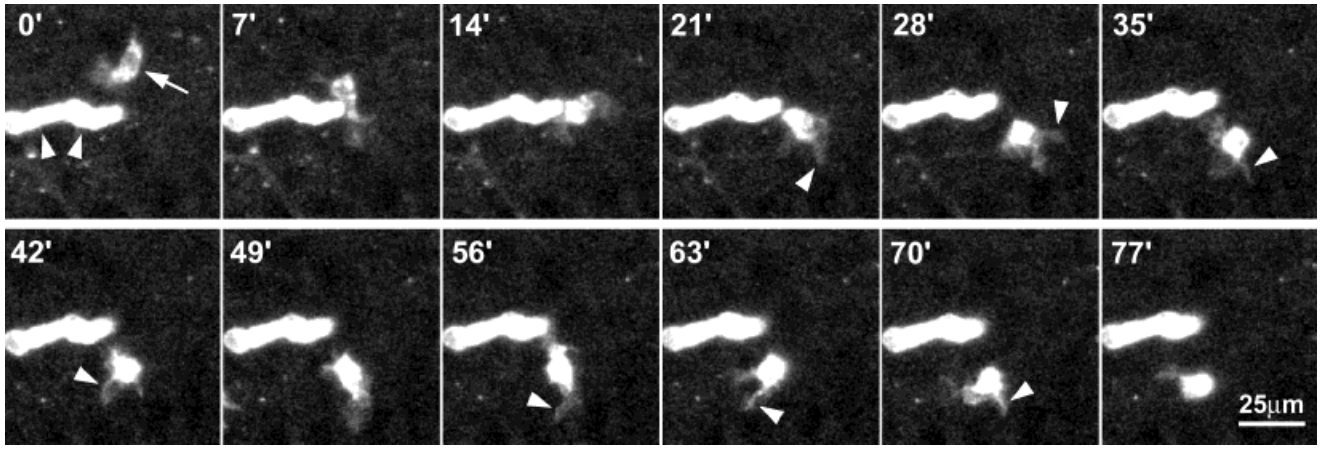

Fig. 7. Locomotory stage. Time sequence of a locomoting microglial cell with multiple lateral protrusions. Over the time period shown, the cell (arrow at 0′) moves through the tissue at a mean rate of 46 μm/h (max rate = 118 μm/h). As it moves, numerous sheet- and cup-like processes (arrowheads at 21′–70′) protrude into the surrounding tissue, presumably contacting many different cells within the time shown. Stereo 3D images (not shown) indicate that the cell passed by the blood vessel (arrowheads at 0′) in a different focal plane and thus probably did not come into direct contact with the vessel. Tissue is from a P4 rat. Images represent a projection of 11 optical sections through 60 μm of tissue depth.

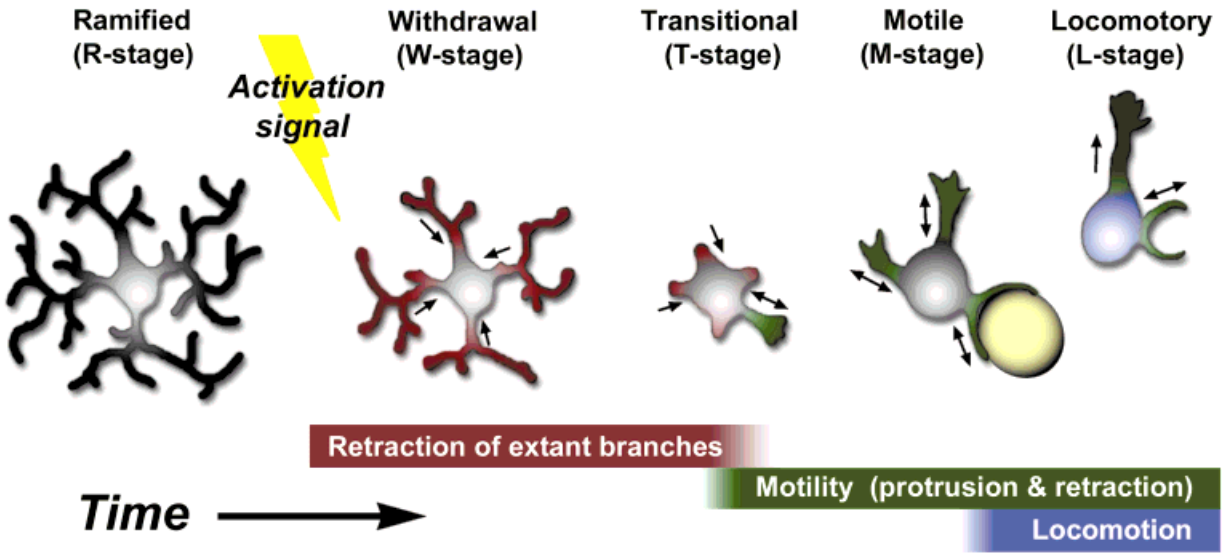

Fig. 8. Multistep model of microglial activation dynamics. Prior to activation, microglia exhibit a highly ramified morphology, with primary branches that can exceed 50 μm in length (R-stage). In response to an activating signal, microglia begin to withdraw the ramified branches (red). During this withdrawal stage (W-stage), there is little or no net extension of processes, only retraction (average withdrawal rate, 0.5–1.5 μm/min). When branches are retracted to within approximately one cell body diameter (~ 10 μm), new protrusions may be generated (green). Microglia in a transitional stage (T-stage) may extend several new protrusions even as the old processes are finally resorbed into the cell body. In the motility stage (M-stage), newly generated protrusions can grow and shrink at rates exceeding 4 μm/min. Some cells do not immediately begin to form new, dynamic protrusions; delays of at least 40 min have been observed between completed branch resorption and formation of new protrusions (e.g., Fig. 2, cell 4). Motile cells begin to contact neighboring cells (yellow) actively. During the locomotory stage (L-stage), microglia can move through the tissue at rates exceeding 110 μm/h. As they do, they transiently contact (frisk) or sometimes engulf other cells.

vated by the slice preparation procedure but were already in a motile form before the brain was removed. However, the present results indicate that hippocampal microglia are indeed activated by the tissue slice preparation procedure, since there was a dramatic and pervasive conversion of nearly all microglial cells from an exclusively ramified form immediately after slicing to an amoeboid form within 12 h after slicing. This is consistent with other studies of long-term hippocampal slice cultures in which microglia were shown to activate and then ultimately revert back to a ramified form within 1–2 weeks in vitro (Hailer et al., 1996, 1997b). Nevertheless, the motile behavior of activated microglia we observed deep within the hippocampal slices is quite similar to that of the presumptive amoeboid microglia observed by Brockhaus et al. (1996).

While it is well established that activated microglia can engulf dead cells and cellular debris, we observed

that they can also transiently ensheathe a cell-sized object, then move on without ingesting the object. We refer to these transient ensheathing events as frisking to indicate their dynamic nature and possible role in tissue surveillance. Although the identity of the frisked objects was not determined here, they are probably neurons or other glial cells, in varying states of health, since the size (10–20 μm) and spheroid shape of the ensheathing profiles approximate that of neuronal and glial cell bodies. Indeed, our hippocampal slices typically contain some dead neurons and glial cells distributed throughout the tissue (Dailey and Waite, 1999), and these are likely targets for microglial interaction. Since phagocytic microglia must distinguish between healthy and dead/damaged cells for removal, frisking may reflect physical screening of neighboring cells for particular cell surface properties. Frisking may also play roles in antigen presentation and the immune response. Ensheathment of damaged cells could allow for efficient uptake of cell surface or diffusible molecules, followed by their presentation to infiltrating lymphocytes (Raivich et al., 1999). Finally, frisking could provide an efficient mechanism for locally removing toxic substances (e.g., glutamate) or delivering protective substances (e.g., neurotrophins) produced by activated microglia (Elkabes et al., 1996; Miwa et al., 1997). Further work will be necessary to determine whether frisking contributes to cytotoxic and/or neuroprotective functions of activated microglia.

We have shown here that the transformation of ramified microglia to amoeboid-like cells is not immediate but instead requires nearly complete resorption of existing branches before the cells exhibit protrusive motility and locomotion. Our time-lapse observations highlight the differences in behavior of preexisting ramified branches and newly generated protrusions. Following activation, the preexisting branches seemed incapable of active extension, and their rate of retraction during the withdrawal phase was generally slower in comparison to that of new protrusions formed during the motility phase. This raises the question of how the dynamic properties of cell protrusions on a single microglial cell may be regulated in space and time. One possibility is that there is a switch in the motile capacity of activated cells that affects all extant protrusions. This would seem consistent with the retraction of all preexisting branches during the withdrawal phase. However, our finding that old and new processes can briefly coexist in the same cell (during the transition phase) while expressing very different dynamic properties (see Fig. 2, cells 5 and 6) would argue against the idea of an immediate, cell-wide change in motility state of all extant processes. Rather, it suggests that the molecular architectures of the old and new processes are distinct, and that these differences confer different motility behaviors. The particular dynamic features of individual cell processes appear to be under strict spatiotemporal regulation.

Two molecular components that are likely to regulate microglial process dynamics are cell adhesion molecules and the cytoskeleton. Changes in expression of integrins or other cell adhesion molecules can alter the character of cell-to-cell interactions (Hynes, 1992; Jones, 1996; Lee and Benveniste, 1999). Hailer et al. (1996) demonstrated that activated microglia in hippocampal slice cultures express the integrin adhesion molecules LFA-1 and VLA-4, whereas ramified microglia do not. Differences in microglial expression of integrins also have been detected following activation in vivo (Akiyama and McGeer, 1990; Hailer et al., 1997a; Kloss et al., 1999; Raivich et al., 1999). Changes in adhesion molecule expression may loosen cell-to-cell contacts made in the resting state, support rapid microglial movement through the tissue, and enable microglia to recognize and interact differently with different cell types (neurons, astrocytes, endothelial cells) or cell states (live, apoptotic, or dead cells).

Microglial branch dynamics are probably also affected by the organization and composition of the underlying cytoskeleton. Preexisting ramified processes may be composed of a more stable cytoskeleton and may thus be incapable of rapid morphological dynamics. Indeed, observations in dissociated cell culture indicate that the branches of ramified microglia are much less dynamic than those of amoeboid cells (Ilschner and Brandt, 1996; Tomita et al., 1996). The ramified cells were shown to contain a higher fraction of detyrosinated and acetylated microtubules (Ilschner and Brandt, 1996), forms that are more stable than unmodified microtubules (Kreis, 1987; Piperno et al., 1987; Webster et al., 1987). Thus, the retraction of ramified branches we observed during the withdrawal phase may depend on depolymerization or fragmentation of a highly stable microtubule lattice. Changes in the vimentin- (Graeber et al., 1988) and actin-based cytoskeleton (Abd-el-Basset and Fedoroff, 1994, 1995; Brockhaus et al., 1996) probably also play important roles in microglial dynamics, but future work will be necessary to clarify the precise roles of the different cytoskeletal systems during activation.

In summary, our results demonstrate that the trauma-induced conversion of resting, ramified microglia to active amoeboid microglia can be rapid (< 2 h), but requires complete withdrawal of ramified branches and formation of a new set of more dynamic protrusions. Further study directed at understanding the molecular basis of this conversion may reveal avenues for regulating microglial function during neuropathological conditions.

ACKNOWLEDGMENTS

N.S. was the recipient of an University of Iowa Medical Student Research Fellowship. Voxblast was developed at the University of Iowa Image Analysis Facility.

REFERENCES

Abd-el-Basset EM, Fedoroff S. 1994. Dynamics of actin filaments in microglia during Fc receptor-mediated phagocytosis. Acta Neuropathol 88:527–537.

Abd-el-Basset EM, Fedoroff S. 1995. Effect of bacterial wall lipopolysaccharide (LPS) on morphology, motility, and cytoskeletal organization of microglia in cultures. J Neurosci Res 41:222–237.

Akiyama H, McGeer PL. 1990. Brain microglia constitutively express beta-2 integrins. J Neuroimmunol 30:81–93.

Aschner M, Allen JW, Kimelberg HK, LoPachin RM, Streit WJ. 1999. Glial cells in neurotoxicity development. Ann Rev Pharmacol Toxicol 39:151–173.

Benati RB, Gehrmann J, Schubert P, Kreutzberg GW. 1993. Cytotoxicity of microglia. Glia 7:111–118.

Booth PL, Thomas WE. 1991. Evidence for motility and pinocytosis in ramified microglia in tissue culture. Brain Res 548:163–171.

Boya J, Calvo JL, Carbonell AL, Borregon A. 1991. A lectin histochemistry study on the development of rat microglial cells. J Anat 175:229–236.

Brockhaus J, Moller T, Kettenmann H. 1996. Phagocytozing ameboid microglial cells studied in a mouse corpus callosum slice preparation. Glia 16:81–90.

Bruce-Keller AJ. 1999. Microglial-neuronal interactions in synaptic damage and recovery. J Neurosci Res 58:191–201.

Dailey ME. 1999. Maintaining live cells and tissue slices in the imaging setup. In: Yuste R, Lanni F, Konnerth A, editors. Imaging living cells. New York: Cold Spring Harbor Laboratory Press. p 10.1–10.7.

Dailey ME, Waite M. 1999. Confocal imaging of microglial cell dynamics in hippocampal slice cultures. Methods 18:222–230.

Dalmau I, Finsen B, Zimmer J, Gonzalez B, Castellano B. 1998. Development of microglia in the postnatal rat hippocampus. Hippocampus 8:458–474.

Davis EJ, Foster TD, Thomas WE. 1994. Cellular forms and functions of brain microglia. Brain Res Bull 34:73–78.

del Rio-Hortega P. 1932. Microglia. In: Penfield W, editor. Cytology and cellular pathology of the nervous system, vol. 2. New York: Paul B. Hoeber. p 481–534.

Elkabes S, DiCicco-Bloom EM, Black IB. 1996. Brain microglia/macrophages express neurotrophins that selectively regulate microglial proliferation and function. J Neurosci 16:2508–2521.

Gähwiler BH, Capogna M, Debanne D, McKinney RA, Thompson SM. 1997. Organotypic slice cultures: a technique has come of age. Trends Neurosci 20:471–477.

González-Scarano F, Baltuch G. 1999. Microglia as mediators of inflammatory and degenerative diseases. Ann Rev Neurosci 22:219–240.

Graeber MB, Streit WJ, Kreutzberg GW. 1988. The microglial cytoskeleton: vimentin is localized within activated cells in situ. J Neurocytol 17:573–580.

Haapaniemi H, Tomita M, Tanahashi N, Takeda H, Yokoyama M, Fukuuchi Y. 1995. Non-amoeboid locomotion of cultured microglia obtained from newborn rat brain. Neurosci Lett 193:121–124.

Hailer NP, Jarhult JD, Nitsch R. 1996. Resting microglial cells in vitro: analysis of morphology and adhesion molecule expression in organotypic hippocampal slice cultures. Glia 18:319–331.

Hailer NP, Bechmann I, Heizmann S, Nitsch R. 1997a. Adhesion molecule expression on phagocytic microglial cells following anterograde degeneration of perforant path axons. Hippocampus 7:341–349.

Hailer NP, Heppner FL, Haas D, Nitsch R. 1997b. Fluorescent dye prelabelled microglial cells migrate into organotypic hippocampal slice cultures and ramify. Eur J Neurosci 9:863–866.

Hynes RO. 1992. Integrins: versatility, modulation, and signaling in cell adhesion. Cell 69:11–25.

Ilschner S, Brandt R. 1996. The transition of microglia to a ramified phenotype is associated with the formation of stable acetylated and detyrosinated microtubules. Glia 2:129–140.

Jones LS. 1996. Integrins: possible functions in the adult CNS. Trends Neurosci 19:68–72.

Kloss CUA, Werner A, Klein MA, Shen J, Menuz K, Probst JC, Kreutzberg GW, Raivich G. 1999. Integrin family of cell adhesion molecules in the injured brain: regulation and cellular localization in the normal and regenerating mouse facial motor nucleus. J Comp Neurol 411:162–178.

Kreis TE. 1987. Microtubules containing detyrosinated tubulin are less dynamic. EMBO J 6:2597–2606.

Kreutzberg GW. 1996. Microglia: a sensor for pathological events in the CNS. Trends Neurosci 19:312–318.

Lee SJ, Benveniste EN. 1999. Adhesion molecule expression and regulation on cells of the central nervous system. J Neuroimmunol 98:77–88.

McGlade-McCulloh E, Morrissey AM, Norona F, Muller KJ. 1989. Individual microglia move rapidly and directly to nerve lesions in the leech central nervous system. Proc Natl Acad Sci USA 86:1093–1097.

Miwa T, Furukawa S, Nakajima K, Furukawa Y, Kohsaka S. 1997. Lipopolysaccharide enhances synthesis of brain-derived neurotrophic factor in cultured rat microglia. J Neurosci Res 50:1023–1029.

Nissl F. 1899. Über einige Beziehungen zwischen Nervenzellenerkrankungen und gliösen Erscheinungen bei verschiedenen Psychosen. Arch Psychiatr 32:1–21.

Piperno G, LeDizet M, Chang XJ. 1987. Microtubules containing acetylated alpha-tubulin in mammalian cells in culture. J Cell Biol 104:289–302.

Raivich G, Jones LL, Kloss CUA, Werner A, Neumann H, Kreutzberg GW. 1998. Immune surveillance in the injured nervous system: T-lymphocytes invade the axotomized mouse facial motor nucleus and aggregate around sites of neuronal degeneration. J Neurosci 18:5804–5816.

Raivich G, Bohatschek M, Kloss CUA, Werner A, Jones LL, Kreutzberg GW. 1999. Neuroglial activation repertoire in the injured brain: graded response, molecular mechanisms and cues to physiological function. Brain Res Rev 30:77–105.

Smith SJ, Cooper M, Waxman A. 1990. Laser microscopy of subcellular structure in living neocortex: can one see dendritic spines twitch? In: Squire LR, Lindenlaub E, editors. XXIII Symposia Medica Hoechst: the biology of memory. Stuttgart: Schattauer Verlag. p 49–71.

Stoppini L, Buchs P-A, Muller D. 1991. A simple method for organotypic cultures of nervous tissue. J Neurosci Methods 37:173–182.

Streit WJ, Kreutzberg GW. 1987. Lectin binding by resting and reactive microglia. J Neurocytol 16:249–260.

Streit WJ. 1990. An improved staining method for rat microglial cells using the lectin from *Griffonia simplicifolia* (GSA I-B4). J Histochem Cytochem 38:1683–1686.

Takeda H, Tomita M, Tanahashi N, Kobari M, Yokoyama M, Takao M, Ito D, Fukuuchi Y. 1998. Hydrogen peroxide enhances phagocytic activity of ameboid microglia. Neurosci Lett 240:5–8.

Thomas WE. 1992. Brain macrophages: evaluation of microglia and their functions. Brain Res Rev 17:61–74.

Tomita M, Fukuuchi Y, Tanahashi N, Kobari M, Takeda H, Yokoyama M, Ito D, Terakawa S. 1996. Swift transformation and locomotion of polymorphonuclear leukocytes and microglia as observed by VEC-DIC microscopy (video microscopy). Keio J Med 45:213–224.

Ward SA, Ransom PA, Booth PL, Thomas WE. 1991. Characterization of ramified microglia in tissue culture: pinocytosis and motility. J Neurosci Res 29:13–28.

Webster D, Gundersen G, Bulinski J, Borisy G. 1987. Differential turnover of tyrosinated and detyrosinated microtubules. Proc Natl Acad Sci USA 84:9040–9044.